THE JOURNAL OF PHYSICAL CHEMISTRY B

Article

pubs.acs.org/JPCB

Conformational Exploration of Two Peptides and Their Hybrid Polymer Conjugates: Potentialities As Self-Aggregating Materials

Nurit Haspel,*[,1] Adèle D. Laurent,[2] David Zanuy,[2] Ruth Nussinov,[3,4] Carlos Alemán,[2,5] Jordi Puiggalí,[2] and Guillem Revilla-López*[,2]

[1]Department of Compuer Science, University of Massachusetts, Boston, Boston, Massachusetts 02125, United States

[2]Departament d'Enginyeria Química, E. T. S. d'Enginyeria Industrial de Barcelona, Universitat Politècnica de Catalunya, Diagonal 647, Barcelona E-08028, Spain

[3]Basic Research Program, SAIC-Frederick, Center for Cancer Research Nanobiology Program, NCI-Frederick, Frederick, Maryland 21702, United States

[4]Department of Human Genetics and Molecular Medicine, Sackler Faculty of Medicine, Tel Aviv University, Tel Aviv 69978, Israel

[5]Center for Research in Nano-Engineering, Universitat Politècnica de Catalunya, Campus Sud, Edifici C', C/Pasqual i Vila s/n, Barcelona E-08028, Spain

ABSTRACT: In this work we elucidate the conformational preferences of two amyloid-forming peptides, Arginine-Vasopressin and Neuromedin-K, and two new biomacromolecular conjugates obtained by linking the two peptides to a polyester (poly(*R*-lactic acid)) chain. The conformational properties of the new hybrid conjugates have been assessed through molecular dynamics simulations and compared to those of their individual components. Our results suggest that the free unconjugated peptides tend to adopt backbone arrangements which resemble a β-hairpin shape, a conformation which has been reported to facilitate amyloid self-aggregation. The backbone conformational preferences of the unlinked peptides are maintained in the peptide−polymer hybrid. Yet significant differences in the side-chains nonbonding interactions patterns were detected between the two states. This suggests that the conformational profile of the peptides' backbones is preserved when linked to the polymer, maintaining the amyloid precursor-like structure. Additionally, several hydrodynamic parameters were computed for both the polylactic acid and for the conjugates: no significant differences were observed, which suggests that the peptide moiety of the hybrid does not significantly affect the conformational tendencies of the polymer chain. Combined, our results provide a conformational exploration of two amyloid-forming peptides and first steps toward the design of two feasible self-aggregating hybrid materials.

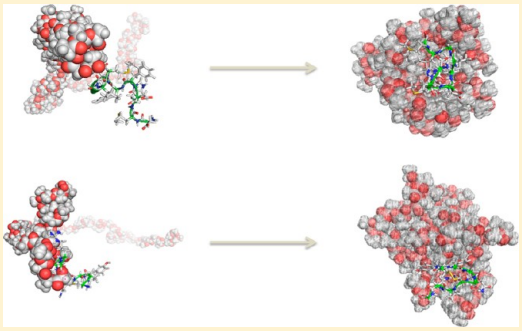

1. INTRODUCTION

Hybrid materials are one of the most active areas in biomaterials science. This is because by combining different types of molecules it is possible to merge their properties into new useful chimeric compounds. The conformational profile of these hybrid compounds has a crucial importance due to its influence on many other parameters such as binding affinity, bioactivity, stability, etc. The conformational landscape of new macromolecules cannot be understood only in terms of a simple addition of their parts; rather, the dynamic interactions between them should also be considered. Thus, conformational exploration needs to be carried out for the whole system and for its separate components, and the results have to be compared. The huge number of feasible combinations of the conformational states of each of the molecular components dramatically increases the complexity of the problem. Theoretical chemistry tools provide a feasible approach for conformational exploration, since they allow performing the search in a faster, more efficient manner. Diblock copolymers that covalently link proteins and synthetic polymers are among the most promising chimeras, being the subject of intense research on both the synthetic[1−4] and the theoretical[5] levels.

Self-aggregating proteins are found in several pathological processes[6,7] and are also an increasing target of research in material science due to their ability to spontaneously form ordered materials with interesting physicochemical and mechanical properties.[5,6] Arginine-Vasopressin (hereafter Vas) and Neuromedin-K (also known as Neurokinin B, and hereafter abbreviated Neuro) are among those peptides that are known to self-aggregate. Vas is a peptidic human hormone involved in the pathogenesis of neurohypophyseal diabetes insipidus (NDI) by aggregating into amyloid-like microfibrils;[7,8] Neuro is a member of the tachykinins protein family that plays an important role as a neurotransmitter and neuroregulator with

Received: May 4, 2012
Revised: November 8, 2012
Published: November 16, 2012

the ability to form fibrils resembling amyloids.[8] Neuro has been shown to decrease neuronal damage caused by β-amyloid protein aggregation by interfering in this molecular process.[9] These two peptides have an intrinsic ability to form self-aggregating self-structured biomaterials[8] both in vivo and in vitro; however, immunological problems may arise due to their proteinogenic nature. On the other hand, poly(*R*-lactic acid) (*R*-PLA, also known as PDLA) is a semicrystalline biodegradable and biocompatible polyester that has physicochemical properties suitable for making release-controlled systems[10] and tissue engineering scaffolds.[11] These features make *R*-PLA a suitable candidate for introducing biocompatible components by conjugating it to these other molecules. Formation of hybrid conjugates by combining peptides (and proteins) with synthetic polymers result in chimeras (i.e., artificial biomolecules) with a useful set of features, where each component has different sets of properties. The capability of peptides and proteins to self-organize into supra-molecular arrangements complements the inherent tendency of *R*-PLA to similarly self-organize at the supra-molecular level. This polyester has a crystallinity of around 37%, a glass transition temperature between 60 and 65 °C, and a melting temperature between 173 and 178 °C.[12] The fusion of such properties may lead to novel macromolecules capable of self-aggregation and self-organizing while preserving the key properties of biodegradability and biocompatibility.[3,11,13]

In this work we use theoretical and computational methods to characterize the conformational preferences of two new hybrid materials derived from the fusion of Vas and Neuro with a 150 residue long *R*-PLA chain. Ascertaining the conformational preferences is a key question for peptide-mediated self-aggregation since the conformations of the individual peptides have a strong impact on their aggregation. This work focuses on noncovalent self-aggregation involving tight binding to a hairpin-like backbone conformation that enables amyloid formation. Thus, the conformational profile of the free peptide is first assessed so it can be compared with the conformational profile of the PLA-linked peptide. The comparison between the free peptide and a peptide linked to a model polymer provides an initial benchmark for studying novel potentially self-aggregating materials. Our approach relies on the premise that a similar conformational behavior of both the free and the polymer-linked peptides is expected to lead to similar properties. Next we investigate the properties of the polymer when isolated and when conjugated to the peptide to ascertain that it also retains its global properties. Here, we present the conformational characterization of two amyloid-genic peptides and two new chimeric molecules combining the properties of amyloidgenic peptides and polymers.[14−18] The study of these specific cases allows us to model new peptide-polymer chimeras based on the general trends observed in studies such as the one presented here. This work sets the path for further theoretical and experimental work to address the peptide and polymer self-aggregation.

2. METHODS

Two peptides with a known tendency to form amyloid-like fibrils both in vitro and in vivo were selected: Neuro and Vas (see Scheme 1). The polymeric moiety of the hybrid molecule was a 150 residues-long tail of *R*-PLA linked to the C-terminus of the peptide. The length of the polymeric chain has been chosen to reproduce the chemical environment of the available literature of experimentally studied hybrid materials.[19] First, the

Scheme 1

CYS-TYR-PHE-GLN-ASN-CYS-PRO-ARG-GLY Arg-vasopressin

ASP-MET-HIS-ASP-PHE-PHE-VAL-GLY-LEU-MET Neuromedin-K

energy landscape of the two free peptides was explored. At subsequent stages, the conformational behavior of the hybrid molecules was similarly studied, using molecular dynamics (MD) simulations at constant volume and temperature (NVT).

All simulations described in this manuscript were performed by using AMBER ff03 force field from the AMBER 9.0[20] program unless other conditions are explicitly expressed. The Berendsen thermostat-barostat[21] was used to control temperature and pressure, with a relaxation time of 1 ps, and the SHAKE[22] algorithm was applied to bonds involving hydrogen atoms. The integration time step was set to 2 fs. The cutoff distance for nonbonding interactions was 14 Å. Particle Mesh of Ewald (PME)[23] was applied for computing electrostatic interactions beyond the cutoff distance. The real space term was determined by the van der Waals cut off (14 Å), whereas the reciprocal term was estimated by interpolation of the effective charge into a charge mesh with a grid thickness of one point per cubic Å. Periodic boundary conditions were applied in all simulations in this paper using the nearest image convention.

Conformational Exploration of Vas and Neuro as Free Peptides. The sequences of the two peptides were extracted from Maji et al.[8] The molecules were solvated with explicit water molecules (approximately 4000 and 3000 for Neuro and Vas, respectively) and their charges neutralized by adding 1 Cl^- and 3 Na^+ for Neuro and 2 Cl^- and 1 Na^+ for Vas. The equilibration protocol consisted of the following: initially, the potential energy of the system was minimized for 2000 steps using steepest descent algorithm. Next, the system was heated up to 500 K during 500 ps in a NVT-MD simulation. After this, 500 ps at 298 K of NVT-MD were run. Finally, 500 ps of NPT-MD were run for density relaxation. The box size was optimized until the density of the system reached 1 g cm^{-3}. The simulation boxes were orthorhombic with sizes of 62 × 55 × 42 Å for Neuro and 52 × 43 × 46 Å for Vas. The TIP3P solvent model was used in all simulations performed in this work.[24] The simulations were performed using NAMD.[25]

The conformational profile of the two peptides was assessed through a simulated annealing (SA) protocol.[26,27] This protocol used the final outputs of the density relaxation and heated them to 900 K and cooled them to 500 K over 10 ns, saving a snapshot every 2 ps (5000 per cycle), and the potential energy of the obtained structures was relaxed through 500 steps of conjugate gradient minimization in order to resolve minor clashes and reach a nearby local minimum. The five lowest potential energy conformations were selected as starting points for the next round. The protocol was run for 5 rounds with 25 000 structures being obtained for each peptide.

The generated structures were clustered based on the phi and psi dihedral angle values and backbone atoms RMSD. The clustering was performed using the K-means clustering protocol.[28] The optimal number of clusters for each peptide was determined to be 200 and 100 for Neuro and Vas, respectively, in order to maintain the intracluster RMSD value above the minimum RMSD value found for the pairwise comparison among the 25 000 structures.

dx.doi.org/10.1021/jp3043363 | J. Phys. Chem. B 2012, 116, 13941−13952

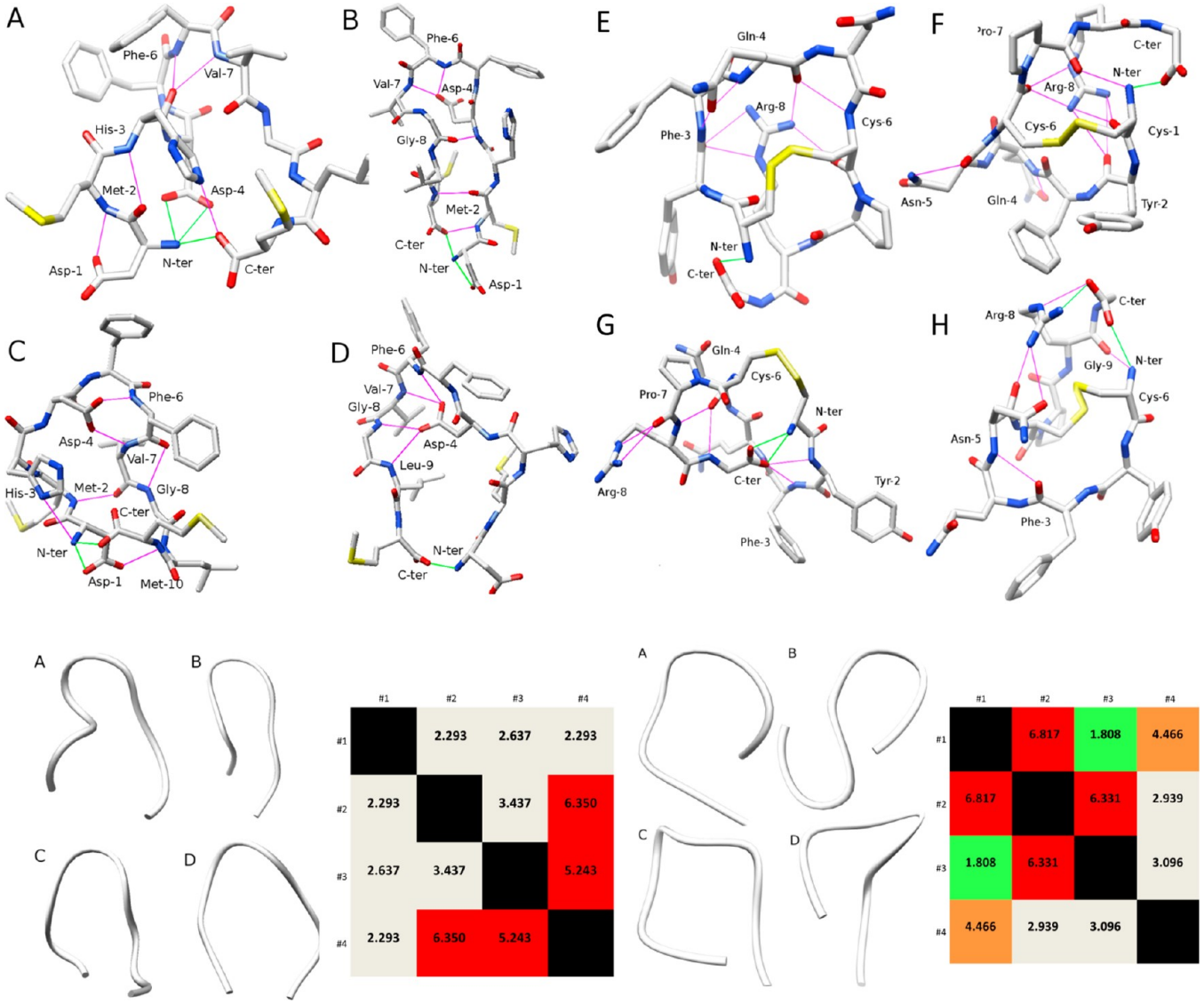

Figure 1. Representation of the four low-energy sructures found in the clustering analysis for Neuromedin-K (A-D) and Arginine-Vasopressin (E-H) as free peptides. Intra main chain noncovalent interactions are represented. Cartoon representations of the backbone are presented in the lowest half of the figure altogether with pairwise intraminima (ordered from lowest to highest energy) backbone RMSD values.

We have chosen an SA protocol for the conformational exploration of the free peptides since this method has proven useful for conformational exploration of peptides in solution.[27] These advantages include the ability of the method to overcome high potential energy barriers and to proficiently explore flat potential energy surfaces compared to plain molecular dynamics (MD) due to its high dependence on the initial geometry.[29] To explore the long-term stability of the lowest energy structures found in the clustering at room temperature (298 K), 20 ns of NVT-MD simulations were later performed by using the 4 lowest energy structures of Neuro and Vas (see Figure 1) as starting structures.

Conformational Exploration of Vas and Neuro Chimeras. Each of the two simulated hybrid systems consisted of the peptide covalently linked to a 150 residue-long *R*-PLA (1.08×10^4 Da) chain. A special force field parametrization was obtained for *R*-PLA to better depict the behavior of the ester linkage.[29] Simulations were made in an orthorhombic box of $201 \times 143 \times 196$ Å and $197 \times 147 \times 197$ Å for Neuro and Vas, respectively. The water molecules were represented explicitly and the total number of atoms was 557 943 and 518 550 for the Neuro and Vas conjugates, respectively. The fully extended conformation was considered for all dihedrals involving the peptide and a random partially folded conformation was considered for the polymer. Density equilibration was performed following the aforementioned protocol but with 1 ns time length for each step. After density relaxation, 30 ns of NVT-MD simulation were performed, with snapshots of the system stored each 2 ps in the accumulated trajectory for the subsequent analyses.

Structural Analysis Parameters. The main criteria used for hydrogen bonds in all structural analyses were a cutoff distance of 3 Å between donor and acceptor atoms and more than 120° for the angle formed between the donor and the acceptor atoms. Salt bridges were considered when the distance between the two charged centers fell below 4 Å. The software used for these analyses were VMD31 and UCSF Chimera[32] and AMBER 9.0[20] package module PTRAJ for the trajectory analysis.

dx.doi.org/10.1021/jp3043363 | *J. Phys. Chem. B* 2012, 116, 13941−13952

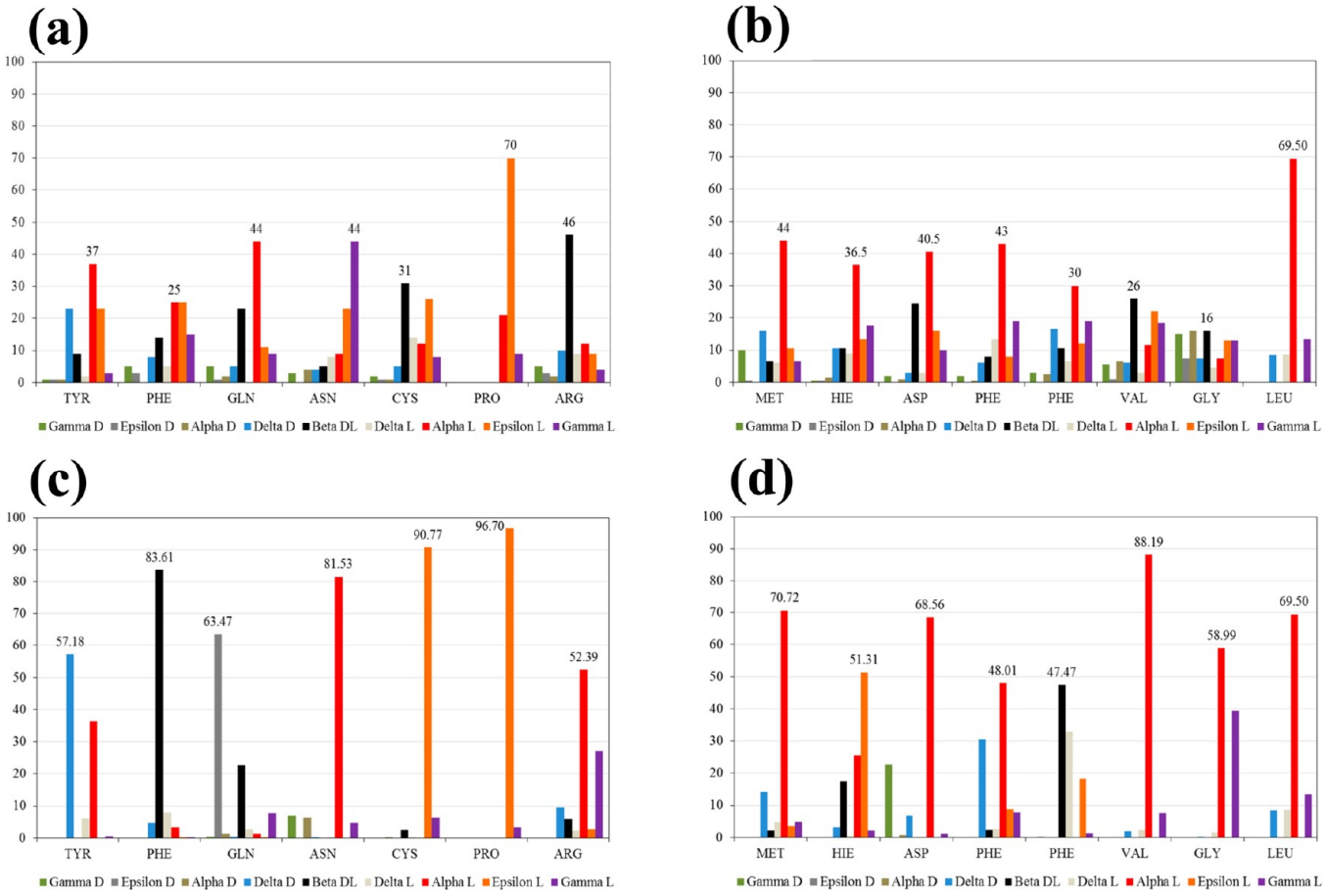

Figure 2. Phi and psi dihedral angle distribution according to Perczel's classification for the 200 clustered structures of Neuro (a) and the 100 clustered structures of Vas (b). Phi and psi dihedral angle distribution according to Perczel's classification for the accumulated values for 30 ns trajectory of Neuro (c) and Vas (d). The highest value is expressed for each amino acid in every case.

3. RESULTS AND DISCUSSION

Conformational Exploration of Vas and Neuro as Free Peptides. First, the SA protocol was used first to study the conformational preferences of the two free peptides in aqueous solution. The analysis indentified 200 representative clusters for Neuro and 100 for Vas. The average number of structures per cluster of Neuro is 125 ± 36 and 225 ± 164 for Vas. The first quartile of clusters was within 20 and 46.8 kcal mol^{-1} for Vas and Neuro, respectively, compared to the detected lowest energy structure. This potentially indicates low structural variability for Vas. This assumption is based on the fact that the probability of a state to exist at a certain temperature can be expressed as a function of the energy difference between that state and the lowest energy state through a Maxwell–Boltzmann distribution. Moreover, a small number of states within an energy range indicates fewer thermodynamically accessible structures at a given temperature and consequently a low conformational variability in terms of energy.

The results for Vas must be taken into consideration carefully since the self-aggregation described for Vas in ref 7 is based on disulfide link formation between different peptides. Disulfide bonds are not only observed to favor aggregation by covalent linkage, but also by retaining the peptide in conformations optimal for noncovalent aggregation.[32]

Figure 1 presents the four structures with the lowest energy cluster centers found in the conformational search of the two peptides together with the main intrachain noncovalent interactions present in these minima. The main conformational preference of these structures is the hook-like shaped partially folded conformations adopted by the backbone. These arrangements are considered among the potential precursors of amyloid-like aggregation since they enable the formation of a cross-β sheet structure. It is also noticeable that for Neuro the lowest energy minima are stabilized by intrachain hydrogen bonds and salt bridges between charged and polar groups of the peptide. For Vas there is a similar main chain conformational tendency, though, in this case, it is bolstered by the disulfide bridge present between cysteine residues (Scheme 1).

Nonbonding interactions (hydrogen bonds and polar and salt bridges) occurring in over 10% of the representative structures of the clusters and backbone arrangements can be seen in Figures 2 and 3. The 10% occurrence threshold is selected since short peptides show great conformational variability. For this reason we set the threshold for nonbonding interactions to be high enough to ensure that those interactions are truly representative and influence the conformational profile of the peptide.[33] Among the specific interactions found in the four representative structures resulting from the cluster analysis of the free Neuro we detect a C-terminus–N-terminus interaction, which helps the backbone to adopt the aforementioned partially folded hook shape. However, the salt bridge between the two termini occurs in less than 10% of all of the structures of the cluster. The structures also present an interaction between the main chain (MC) or side chain

dx.doi.org/10.1021/jp3043363 | J. Phys. Chem. B 2012, 116, 13941–13952

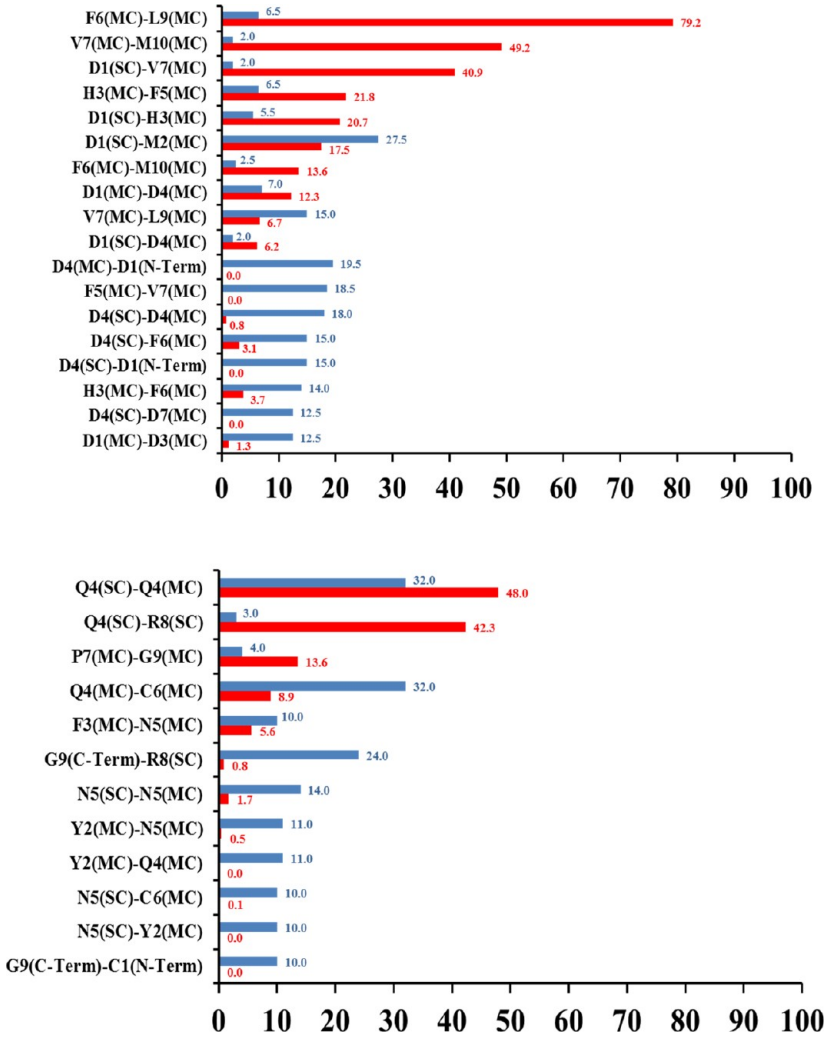

Figure 3. Percentage of hydrogen bonds and salt bridges with an occurrence over 10% for the Neuro (a) and Vas (b): red bars are for PLA-linked peptides and blue bars are for free uncapped peptides. The geometric criteria is a distance lower than 3.5 Å and an angle higher than 120°. SC and MC refer to side chain and main chain, respectively.

(SC) of the Aspartate residue in position four with the N-terminus of the peptide which occurs in around 19% (D4MC−D1 N-term) and 15% (D4 SC−D1 N-term) of the structures, respectively. This contact is expected to help stabilizing the hook shape in a way similar to the interaction between the two charged termini. A detailed analysis of the nonbonding interactions between the polar groups of the peptide backbone reveals 8 hydrogen bonding interactions between different amino acids having an occurrence of over 5% (see Figure 3). Four of them follow an $i \rightarrow i + 2$ pattern, while the other four are involved in an $i \rightarrow i + 3$ pattern. These two patterns correspond to γ-turn and 3/10 helix motifs, respectively, and both are present in the backbone arrangements which have a turn motif, supporting our initial observations.

The analysis of the four structures with the lowest energy in the Vas clusters also shows that the interactions between the free termini of the peptide are a key feature. In the 200 representative structures resulting from the clustering, the salt-bridge between the termini is present with an occurrence of 9%. This finding does not agree with that of Neuro and can be explained by the restriction of backbone mobility induced by the disulfide bridge between the cysteine residues, which facilitates the adoption of the partially folded conformations similar to the ones detected in the four lowest energy minima.

The 5 different interactions between polar groups of the backbone with an occurrence over >5% among the 200 representative structures of Vas can be sorted into two patterns: 4 follow an $i \rightarrow i+2$ pattern and 1 follows an $i \rightarrow i + 3$. The high variability found among the representative clustered structures of the two peptides can be explained not only by the great energy gaps between clusters that leaves as representative just a few of the structures (making the rest irrelevant) but also by the inherent variability associated with side-chain interactions and backbone arrangements in peptides as was observed in the literature,[28] as well as inaccuracies of the clustering method.

The conformational flexibility detected for the four lowest energy structures of the two peptides is expected to play an important role in amyloid formation. This can be assessed by the pairwise backbone RMSD values in Figure 1. The range of values for the peptide backbone RMSD varies between 2.29 and 6.35 Å for Neuro and between 1.81 and 6.82 Å for Vas. These intervals confirm that Vas has a restricted conformational profile in comparison to Neuro and establish a benchmark to compare the structures found for both peptides. In addition,

dx.doi.org/10.1021/jp3043363 | J. Phys. Chem. B 2012, 116, 13941−13952

conformational flexibility has been identified as a key factor to explain amyloid formation. The partially unfolded structures with an initial high conformational variability accommodate the nonbonding interactions (electrostatic and van der Waals) and form the precursors of the amyloid filaments. Once these precursors are formed, a decrease in conformational variability combined with an increase in the occurrence of β-strand conformations takes place. This leads to the organization of supra-molecular structures such as amyloid protofilaments.[34,35]

The Perczel's regions[36] distribution for the amino acids of Vas and Neuro can be seen in Figure 2a,b, respectively. The data suggest that conformations associated with helical and/or turn motifs are clearly dominant, however, a significant portion of the conformations reside in the β_{DL} region (the one that includes β-strand conformation). This is in agreement with the aforementioned nonbonding interaction patterns that suggest the turn arrangements for the most representative backbone conformations.

For Neuro (Figure 2b), five of the eight central amino acids presented the α_L region (right-handed α-helix) as the most populated, and in three of them the β_{DL} was the most populated. Helical amino acids are more frequent in the N-terminal region or close to it, whereas β_{DL} residues are in the C-terminal region. This trend is consistent with the tendency of the N-terminal region to show a more disordered organization (rather than a β-strand conformation) as reported in the literature for other amyloidogenic proteins.[35]

Analysis of the seven central amino acids of Vas according to Perczel's secondary structure classification indicates that three residues adopt α_L, one adopts ε_L, one γ_L, and two β_{DL} (Figure 2a). Helical conformations are again concentrated in the N-terminal region while semiextended conformations are in the C-terminal region. However, in this case, residues with a semiextended backbone alternate with others with a turn disposition (ε_L and γ_L) for the backbone.

MD Simulations of Free Vas and Neuro. Since the simulated annealing-based conformational search was performed at high temperature to help escape local minima, we set out to test whether the low-energy minima we discovered are stable over time at room temperature. We simulated the four Neuro and four Vas lowest energy representative structures found in the clustering analysis (shown in Figure 1) at 298 K and 1g cm^{-3} density for 20 ns each.

Figure 4a shows the total potential energy and Figure 4b shows the backbone RMSD with respect to the initial conformation of the four Neuro energy minima. The structures are denoted according to their index in Figure 1. The lowest energy system corresponds to the configuration shown in Figure 1b. It was remarkably structurally stable, with an average backbone RMSD of less than 1.5 Å during the simulation. Figure 5 shows snapshots of the initial structure and the trajectory after 10 and 20 ns. As seen, the structure is well maintained and the peptide assumes a hairpin-like conformation for all simulated times. These results mean that this conformation, highly accessible by Neuro, is highly stable when thermal agitation is considered over a long period of time. Consequently, we can conclude that this minimum found as thermodynamically accessible in the simulated annealing conformational search is highly stable at lower temperatures and can be a good starting point for further aggregation studies. The rest of the low energy Neuro conformers were slightly less stable, although most of them, with the exception of 1c, kept their overall organization throughout most of the simulation

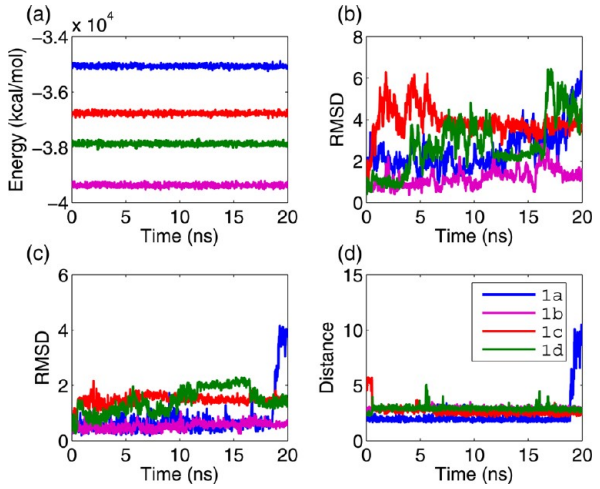

Figure 4. Analysis of the 20 ns MD simulation of the four Neuro energy minima shown in Figure 1. The inset legend refers to the indices of the structures as shown in Figure 1. (a) The potential energy. (b) The backbone RMSD (in Å). (c) The backbone RMSD of residues 3−8 (in Å). (d) The distance (in Å) between the interacting groups of Asp4-Val7 (or Phe3-Val7 in structure 1a).

with RMSD values of 4 Å or less with respect to the initial structure, which is a reasonably low value considering the length of the Neuro peptide.

A closer look at Neuro structures shows that all of them maintained a hairpin-like motif throughout the simulation. This trend is demonstrated even more clearly if the two residues from each terminus are removed from the calculation, since they are less constrained and in such a short peptide this may affect the RMSD significantly, as can be seen in Figure 4d, which shows the backbone RMSD of residues 3−8. In all of the structures the RMSD for residues 3−8 was below 2 Å during most of the simulation time, except structure 1a which reorganized toward the end of the simulation. As discussed above, the most frequently observed interaction is the hydrogen bond between the side chain of Asp4 and the main chain of Val7. This interaction is observed in structures 1b, 1c, and 1d. In structure 1a this interaction does not exist, but there is a hydrogen bond between the main chain of Phe3 and the main chain of Val7. Figure 4d shows the distance between the interacting groups. In all cases, the distance was very stable (between 2 and 3 Å) throughout most or all of the simulation, indicating a strong and stable interaction. This result means that a hydrogen bond between residues 3 or 4 and residue 7 is highly important to maintain the partially folded β-strand organization. The salt bridge between the N and C termini was not observed frequently, and its occurrence was only significant (56% of the snapshots) for structure 1b. Therefore, we can conclude that the lowest energy structures found in the conformational search are also stable under thermal agitation at 298 K despite the variability in the noncovalent interactions. This conclusion reinforces, at the same time, the results of the conformational search by proving the stability of the most accessible structures found in the search for Neuro and by showing a high variability of the nonbonded interactions in contrast with the backbone stability.

Figures 6 and 7 show the results for the MD runs of the four Vas energy minima shown in Figure 1e−h. Figure 6a shows the potential energy; Figure 6b shows the backbone RMSD with respect to the initial structure; and Figure 6c shows the

dx.doi.org/10.1021/jp3043363 | J. Phys. Chem. B 2012, 116, 13941−13952

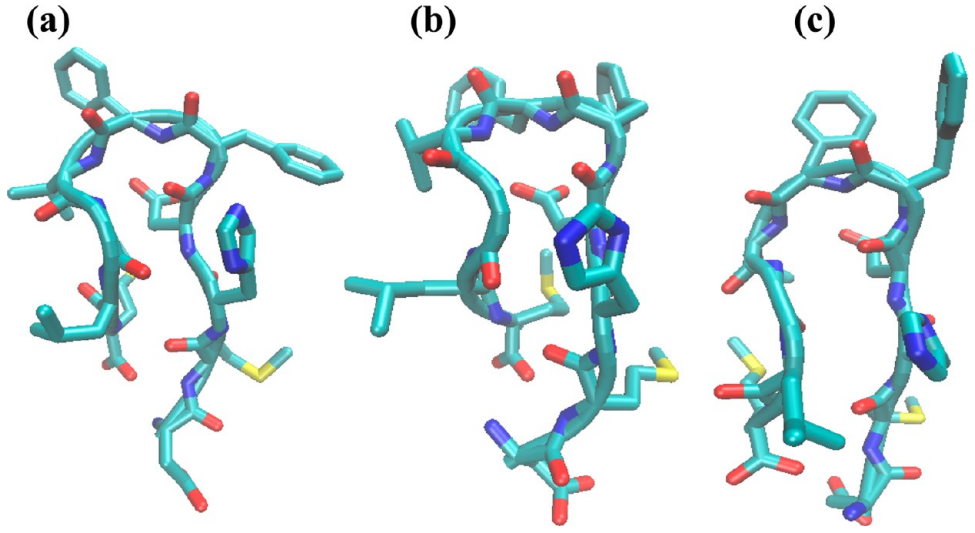

Figure 5. Snapshots of the Neuro 20 ns-trajectory shown in Figure 1b in the beginning of the MD simulation (a), after 10 ns (b), and after 20 ns (c). Hydrogen atoms were omitted and the backbone is traced for clarity.

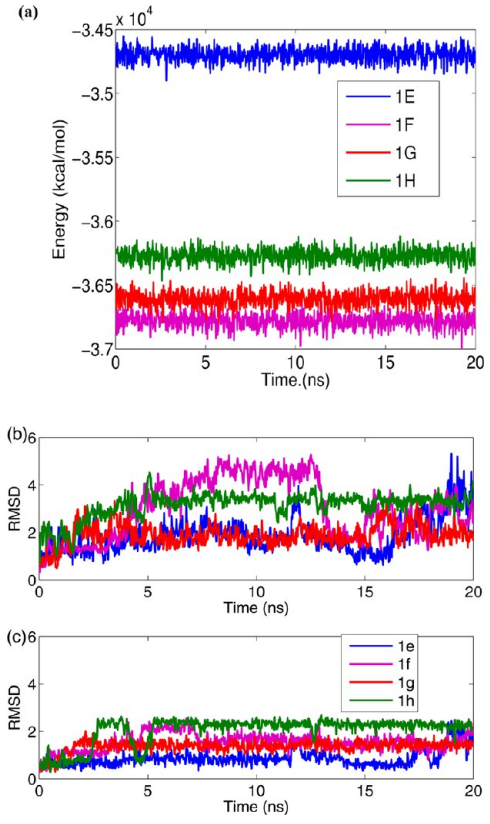

Figure 6. Analysis of the 20 ns MD simulation of the Vas energy minima shown in Figure 1e–g. The inset legend refers to the indices of the conformations shown in Figure 1. (a) The potential energy. (b) The backbone RMSD. (c) The backbone RMSD when only residues 1–7 are considered.

backbone RMSD when only residues 1–7 are considered. The structures are again denoted according to their index in Figure 1. The reason to remove only the C-terminal residues from the RMSD calculation in Figure 6c was that residue 1 (Cysteine) is involved in the disulfide bond, and therefore its conformational variability is not as high as it usually is for a terminal residue. The conformations shown in Figure 1e,g were considerably more stable than the other two. Their overall backbone RMSD was less than 2 Å on average. The region containing residues 1–7 showed more stability in all 4 structures, as can be seen in Figure 7c. Structures 1e and 1g were again the most stable and after initial self-organization both maintained a backbone RMSD below 1.5 Å throughout the simulation. This is not surprising since this region is constrained by the disulfide bond between residues 1 and 6. Figure 6a shows that structure 1g is the second-lowest energy structure, but the difference from the lowest energy structure is small −173 kcal/mol including the solvent molecules. Figure 7 shows snapshots of conformations 1e and 1g in the beginning, after 10 ns, and after 20 ns of the simulation. As in the case of Neuro above, the overall organization of 1g resembles a hairpin-like structure, whereas 1e has a more globular shape, maintained mostly by the intrapeptide disulfide bond. In the case of Vas there were no distinct pairwise interactions preserved across all low energy conformations, as we believe that the disulfide bond is what mostly helps keep the structural organization intact.

Conformational Exploration of PLA-Linked Vas and Neuro. The conformational propensities of the Vas and Neuro peptides linked to a *R*-PLA chain of 150 residues long (hereafter Neuro-PLA and Vas-PLA) were investigated. This model system attempts to assess the impact of the polymer on the conformational preferences of the peptides in the conjugates, in which their respective C-terminus are covalently linked to the polymer chain. It should be noted that these two experiments do not intend to perform full conformational explorations of the hybrid macromolecule. MD simulations starting from a fully extended conformation for both peptide and polymer purportedly attempt to find local minima (thermodynamic traps) adopted by the peptide. The reason to perform these two experiments is to investigate whether the conformational preferences found for the free peptide are reproduced when starting from a fully extended conformation. In order to accomplish the mentioned goals, peptide backbone conformations resulting from the MD trajectory are systematically compared to the lowest energy ones obtained for the free peptides.

Figure 8 compares the temporal evolution of the backbone RMSDs for the peptide linked to PLA, calculated for the four

dx.doi.org/10.1021/jp3043363 | *J. Phys. Chem. B* 2012, 116, 13941–13952

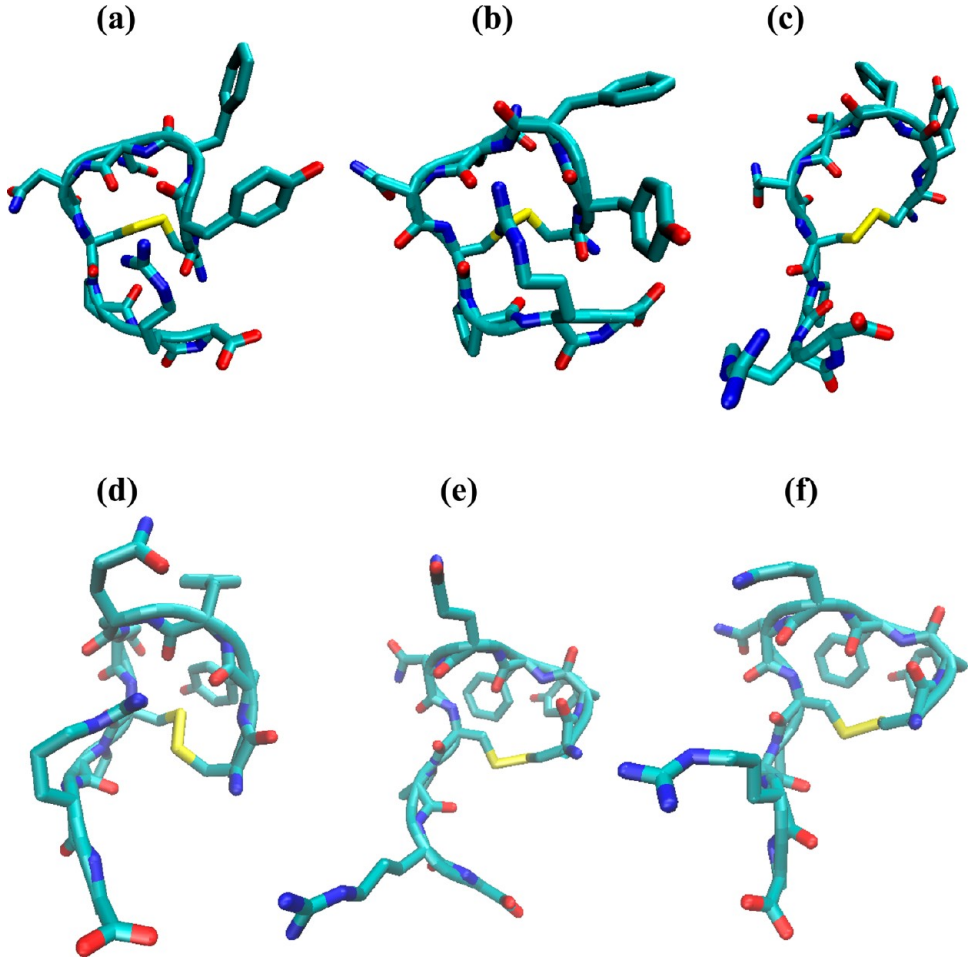

Figure 7. Snapshots of the Vas conformation shown in Figure 1e,g in the beginning of the MD simulation (a and d), after 10 ns (b and e), and after 20 ns (c and f). Hydrogen atoms were omitted and the backbone is traced for clarity.

lowest energy structures found in the clustering. The analysis for the Neuro-PLA suggests a high similarity between the backbones of the peptide linked to the PLA and the four structures with the lowest energy obtained for the free peptide. RMSD values range from 2.5 to 4.5 Å during the 30 ns simulation, indicating that the four most representative backbone arrangements found in the clustering analysis of Neuro are accessible to the peptide when it is a part of a chimera. This latter observation is especially remarkable if we consider that this range (2.5−4.5 Å) falls within the maximum range of RMSD values observed in Figure 1 for the pairwise backbone comparison. Thus, indicating a preference of the peptide moiety toward these structures.

The RMSDs of the Vas-PLA trajectory tends to vary less, ranging from 1 to 4 Å. Moreover, the RMSD comparison displayed in Figure 8b indicates relatively small changes since the preference for the first and third lowest energy representative conformations of the free peptide remains unchanged throughout the last phase of the MD simulation. Putting these data together, we deduce that the main conformational features that should enable self-aggregation in the free proteins are preserved in the hybrid conjugates.

The two previous observations also confirm that the conformational variability of the backbone of the peptides is reduced when they are linked to the polymer chain. Furthermore, the backbone conformational profile of the peptide moiety is indeed similar to that found for the free peptides, as the low RMSD values in Figure 8 prove. This is especially relevant since the exploration of both the free peptide and the linked peptide-polymer started from an extended conformation. Thus, these findings highlight the preference of the polymer-linked peptide to adopt conformations similar to those found for the free molecule. This can be regarded as a consequence of the restricted conformational profiles of the peptide backbones previously found in the simulated annealing conformational exploration. However, it should be mentioned that the 30 ns trajectories of the macromolecular chimeras are not directly comparable to those conformational exploration of the free form. The latter experiment aimed at proving that energetic wells found in the SA protocol were deep enough to even dominate the structural behavior of the peptide in the chimeric macromolecule environment.

Nonbonding interactions between polar and charged groups (Figure 3) may be an important factor not only for stabilizing the conformations but also for the recognition between the molecules during self-assembly. The data for Neuro-PLA reflect dramatic changes compared to Neuro because 9 of the 10 interactions with occurrence of over 10% in the free peptide appear in less than 10% of the conformations or simply disappear. In addition, among the representative interactions in Neuro-PLA only one is present in the free peptide with frequency over 10%. The interactions between the main chain polar groups with occurrences over 5% can be classified into six different interactions depending on the relative position of the

dx.doi.org/10.1021/jp3043363 | J. Phys. Chem. B 2012, 116, 13941−13952

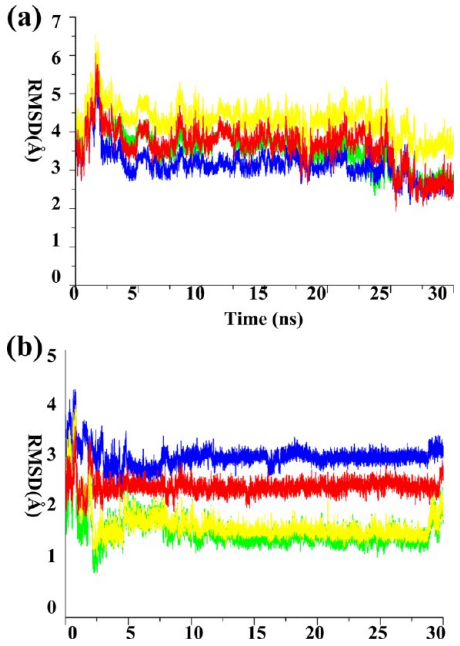

Figure 8. Time evolution of the RMSD values for the 30 ns PLA-linked trajectories of Neuro (a) and Vas (B). The colors represent the reference structure used to calculate RMSD: green, blue, yellow, and red refer to the lowest, second lowest, third lowest, and fourth lowest minimum energy conformation, respectively, of the free peptide.

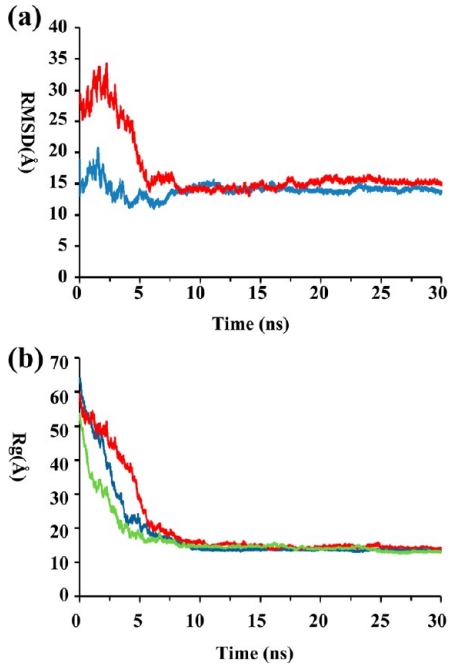

Figure 9. (a) Time evolution of the RMSD for the PLA moiety of the hybrid conjugates through the 30 ns trajectory of Neuro (blue) and Vasopressin (red). RMSDs have been calculated with respect to the free polymer chain. (b) Time evolution of the radius of gyration through the 30 ns trajectory for Neuro (blue) and Vas (red) hybrid conjugates, and *R*-PLA (green).

residues in the peptide chain: three interactions between residues in positions $i \rightarrow i + 2$, two between positions $i \rightarrow i + 3$, and one between positions $i \rightarrow i + 4$. These correspond to γ-turn, 3_{10}-helix, and α-helix motifs, respectively, and represent a reduction in the total number of interactions (eight interactions versus six) and a slight imbalance toward $i \rightarrow i + 3$ regularity in comparison to the free peptide. Vas-PLA depicts a behavior similar to that found for Neuro-PLA: just 1 of the 10 interactions found in the free peptide, with an occurrence of over 10%, is present in the PLA conjugate with a frequency of >10%; and just one out of three interactions found in the chimera is also present (over 10%) in the free peptide. In Vas-PLA there is also more imbalance in the regularity patterns of the representative interactions between backbone polar groups with the $i \rightarrow i + 3$ pattern found in only three cases (four for the free peptide plus one interaction in the $i \rightarrow i + 4$ motif).

These results suggest that PLA disrupts polar and salt bridge interactions of the side chains. This effect can be rationalized if we take into consideration that the peptide needs to accommodate a pocket formed in the polymer bundle (see Figures 9 and 10). This allows the backbone to maintain its conformational preferences; however, it presents difficulties for the side chains to preserve the interactions they had in the free peptide. Thus, although the backbone organization has similar trends, it seems reasonable that the new interactions between the side chains together with the interactions of the main polar groups of the backbone and the peptide-polymer contacts help the peptide to adopt such an organization.

These results are in agreement with the available literature for other hybrid systems where it is clearly shown that the interaction between the peptide and the polymer may have a strong influence on the peptide backbone depending on both the peptide sequence and polymer length.[19] Furthermore, the observed stable backbone conformational preferences of the peptides linked to the polymer, along with their high similarity to those of the free peptide, can be attributed to relatively decreased conformational flexibility of the peptide backbones which tends to adopt some conformations without regard of the polymer moiety effects on side chains plasticity and weak interactions. This observation opens a way for both experimental and computational studies of backbone conformation-related properties such as noncovalent amyloid-like self-aggregation: self-aggregation in the chimeras should be similar to that in the free peptides as long as the backbone arrangements are similar.

Conformational Exploration of PLA. The 150 residues-long PLA chain represents a standard polymer model in the hybrid materials field. However, to the best of our knowledge no covalently linked conjugates between *R*-PLA and an amyloidogenic protein have been studied at the theoretical level though several experimental studies of hybrid systems are available in the literature.[19,37−40]

The conformational behavior of the polymeric moiety can be assessed in terms of different hydrodynamic and structural parameters[41,42] such as radius of gyration (R_g), stokes radius, intrinsic volume, and sedimentation velocities. We have computed these parameters for the three simulated systems (Neuro-PLA, Vas-PLA, and PLA) using the hydropro.7c software[42] for the last 2 ns of simulation, which corresponds to the stationary phase of their respective 30 ns MD-NVT simulations. The results are provided in Figure 9 and Table 1. Figure 9 shows both the temporal evolution of the R_g and the RMSD for the *R*-PLA fragment of the conjugates with respect to the free polymer chain.

As can be seen, the nanoscopic behavior of the polymer is similar for all systems since R_g becomes stationary at around 15 Å for the 30 ns simulations: 14.25 ± 3.14, 15.52 ± 4.52, and 14.41 ± 2.13 Å for Neuro-PLA, Vas-PLA, and PLA, respectively

dx.doi.org/10.1021/jp3043363 | J. Phys. Chem. B 2012, 116, 13941−13952

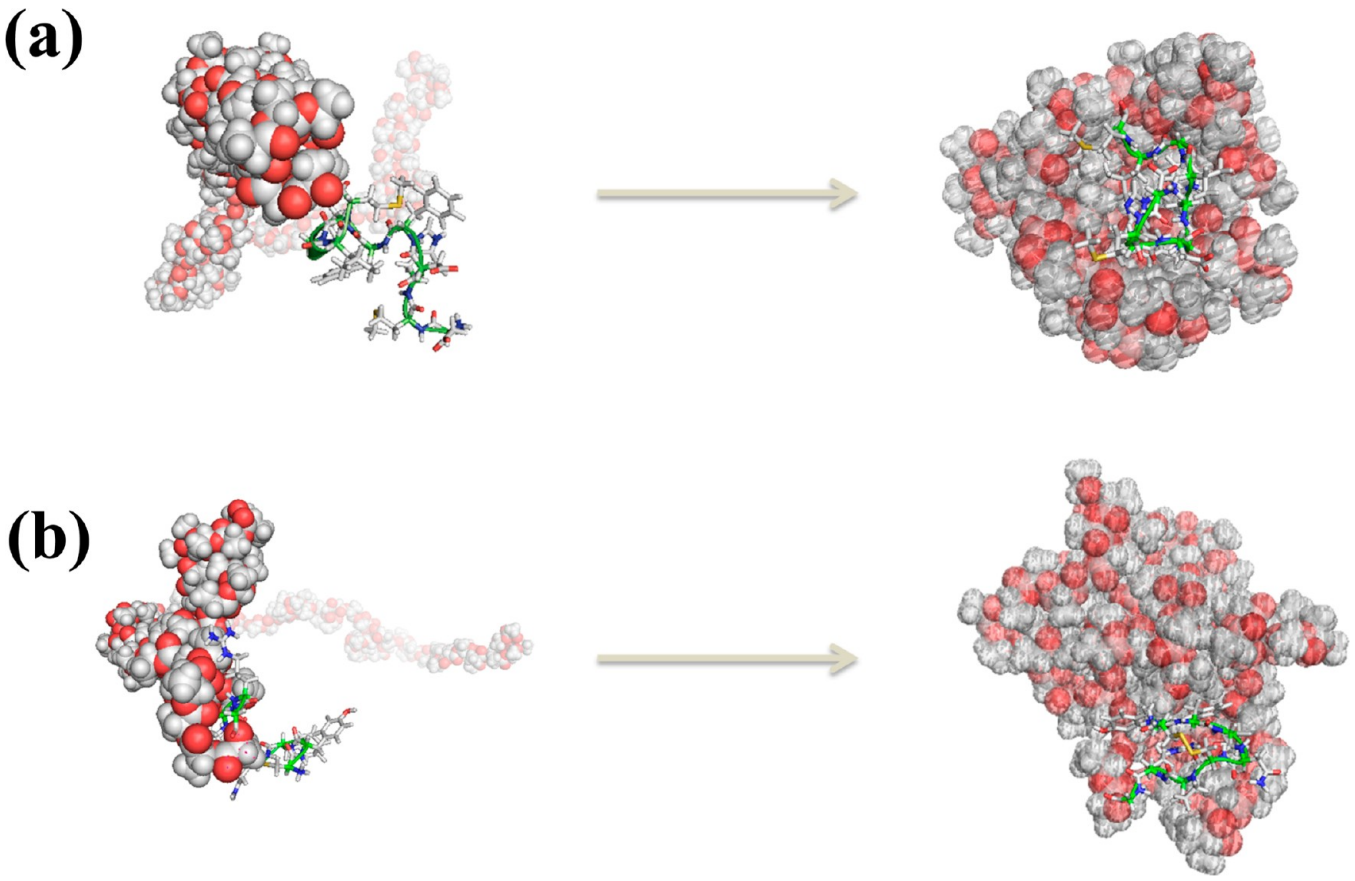

Figure 10. Initial and final snapshot image of the 30 ns long MD-NVT simulation of Neuro-PLA (a) and Vas-PLA (b). *R*-PLA is represented by filled spheres, and the peptide is depicted with sticks and cartoon for the backbone.

Table 1. Selected Hydrodynamical Parameters for the Three Simulated Systems[a]

	R_g (cm)	Stokes radius (cm)	intrinsic volume (cm^3)	sedimentation velocity (Svedbergs)
Neuro-PLA	$1.57 \times 10^{-7} \pm 2.54 \times 10^{-8}$	$2.21 \times 10^{-7} \pm 3.10 \times 10^{-8}$	$2.15 \times 10^{-20} \pm 3.43 \times 10^{-21}$	1.31 ± 0.17
Vas-PLA	$1.79 \times 10^{-7} \pm 4.48 \times 10^{-8}$	$2.22 \times 10^{-7} \pm 2.88 \times 10^{-8}$	$2.11 \times 10^{-20} \pm 2.95 \times 10^{-21}$	1.29 ± 0.15
PLA	$1.57 \times 10^{-7} \pm 4.15 \times 10^{-8}$	$2.10 \times 10^{-7} \pm 2.72 \times 10^{-8}$	$1.95 \times 10^{-20} \pm 2.77 \times 10^{-21}$	1.25 ± 0.15

[a]Data collected from the last 2 ns of a 30 ns trajectory and expressed as average ±2 times the standard deviation. R_g refers to the radius of gyration.

(n = 12500 in each case, 75% confidence interval). Furthermore, we can also conclude that the RMSD variations of the two hybrid systems, which were calculated using the free polymer chain as the reference, are small and nonsignificant for such a big macromolecule. Thus, the average RMSD values (i.e., 13.94 ± 1.33 and 15.03 ± 1.53 Å for Neuro-PLA and Vas-PLA, respectively) represent a tiny atom-averaged value.

The rest of the aforementioned parameters are detailed in Table 1. As can be seen, no statistically relevant differences are observed (significance level of two tail Student T-test (α) of 0.05; n = 1000 for each simulation) over the 30 ns long simulation. The values of all 75% confidence intervals overlap. These data clearly suggest that there is no significant conformational influence neither of the polymer on the peptide nor of the peptide on the polymer as reported in the literature for other peptide-polymer conjugates.[44]

4. CONCLUSIONS

The conformational preferences of two amyloid-forming peptides (Vas and Neuro) were elucidated by using an SA-MD protocol, which has been shown to be valid for the exploration of the conformational landscape of short peptides despite their conformational variability.[27,29,45] Our results indicate that the preferred conformational profile of both peptides, particularly that of Neuro, tend to adopt turn arrangements for the backbone which resemble a β-hairpin shape. This conformation has been identified earlier as potential precursors in self-aggregation. Importantly, earlier observations pointed to the key role of covalent disulfide cross-linking in the self-aggregation of Vas. On the other hand, here we aimed to assess the ability of the peptide to aggregate due to the stabilizing effect of intrachain disulfide bonds (the native state of the peptide) as shown for other proteins.[33] Next, the conformational preferences of two hybrid macromolecules consisting of each of the peptides covalently linked to a 150 residues-long model *R*-PLA chain were studied. They were compared to the preferences of the free peptides to see if the conformational propensities of the precursors of amyloid structure are preserved in the new chimera. This comparison illustrates similar trends for the 3D arrangement of the peptide backbone despite the significant differences which were observed in side-chains interactions. Combined, these results suggest that the conformational profile of the free peptides may

dx.doi.org/10.1021/jp3043363 | J. Phys. Chem. B 2012, 116, 13941−13952

favor noncovalent amyloid aggregation. Moreover, the conformational propensities of the peptides are mostly conserved in the hybrid conjugate thus preserving the potential peptide-mediated amyloid formation in the macromolecule. This latter finding should be considered independently of self-aggregation events which may be mediated by the polymer chain or the covalent cross-linking between sulfhydryl groups of Vas chains.

The effect that the chemically bound peptide may have on the conformational preferences of the polymer has been further investigated by establishing a control system made of a 150 residues-long *R*-PLA chain. The size of the polymeric chain was chosen based on the number of residues in polylactic chains frequently used in experiments. This polymer chain mimics the peptide-polymer interactions in dilute solution; thus, not reproducing the properties of the polymer in neither the solid phase nor a hyper-crowded solution. Comparisons were made between the polymer part of the conjugates and the individual PLA chain in order to qualitatively point out the effects of peptide on polymer. We found that there are no significant differences in the conformational and nanoscopic properties of the polymer with regard to the presence of the covalently linked peptide. Finally, some relevant hydrodynamical properties have been elucidated for the two conjugates. They were compared to those of a single *R*-PLA chain and again showed that no significant difference is present. Thus, overall, the conjugation of amyloidogenic self-aggregating peptides and polyester appears to retain the conformational properties of its components, which is expected to be useful in material design. This work opens the way for future explorations, at both the experimental and theoretical levels, of self-aggregation of hybrid materials derived from molecules with similar chemical properties.

AUTHOR INFORMATION

Corresponding Author

*E-mail: nurit.haspel@umb.edu; guillermo.revilla@upc.edu.

Notes

The authors declare no competing financial interest.

ACKNOWLEDGMENTS

This work has been supported by MICINN and FEDER (Grants MAT2009-09138 and MAT2009-11503), by the Generalitat de Catalunya (Grants 2009-SGR-925, 2009SGR-1208, and XRQTC), and by the UMass Boston proposal development grant (N.H). The authors are indebted for the computational resources provided by "Centre de Supercomputació de Catalunya" (CESCA), Barcelona Supercumpting Center (BSC, Project QCM-2011-2-0020) and the high-performance computational capabilities of the Biowulf Linux cluster at the National Institutes of Health, Bethesda, Md. (http://biowulf.nih.gov). Part of the calculations were carried out on the supercomputing facilities in the College of Science and Mathematics at UMass Boston. Support for the research of C.A. was received through the prize "ICREA Academia" for excellence in research funded by the Generalitat de Catalunya. The research was supported in part by the National Science Foundation through TeraGrid resources provided by the Texas Advanced Computing Center (TACC) under Grant No. TG-MCB100025 (N.H.). This project has been funded in whole or in part with Federal funds from the National Cancer Institute, National Institutes of Health, under Contract No. HHSN261200800001E. The content of this publication does not necessarily reflect the views or policies of the Department of Health and Human Services, nor does mention of trade names, commercial products, or organizations imply endorsement by the U.S. Government. This research was supported (in part) by the Intramural Research Program of the NIH, National Cancer Institute, Center for Cancer Research.

REFERENCES

(1) Velonia, K. *Polym. Chem-UK* **2010**, *1*, 944−952.
(2) Börner, H. G. *Macromol. Rapid Commun.* **2011**, *32*, 115−126.
(3) Börner, H. G.; Schlaad, H. *Soft Matter.* **2007**, *3*, 394−408.
(4) Rosler, A.; Klok, H. A.; Hamley, I. W.; Castelletto, V.; Mykhaylyk, O. O. *Biomacromolecules* **2003**, *4*, 859−863.
(5) Shaytan, A. K.; Khokhlov, A. R.; Khalatur, P. G. *Soft Matter.* **2010**, *6*, 1453−1461.
(6) Carrell, R. W.; Lomas, D. A. *Lancet.* **1997**, *350*, 134−138.
(7) Birk, J.; Friberg, M. A.; Prescianotto-Baschong, C.; Spiess, M.; Rutishauser, J. *J. Cell Sci.* **2009**, *122*, 3994−4002.
(8) Maji, S. K.; et al. *Science* **2009**, *325*, 328−332.
(9) Flashner, E.; Raviv, U.; Friedler, A. *Biochem. Bioph. Res. Co.* **2011**, *407*, 13−17.
(10) Brannon-Peppas, L. *Int. J. Pharmaceut.* **1995**, *116*, 1−9.
(11) Vandermeulen, G. W. M.; Klok, H. A. *Macromol. Biosci.* **2004**, *4*, 383−398.
(12) Sodergard, A.; Stolt, M. *Prog. Polym. Sci.* **2002**, *27*, 1123−1163.
(13) Rabotyagoba, O. S.; Cebe, P.; Kaplan, D. L. *Biomacromolecules* **2011**, *12*, 269−289.
(14) Cherny, I.; Gazit, E. *Angew. Chem., Int. Ed.* **2008**, *47*, 4062−4069.
(15) Reches, M.; Gazit, E. *Science* **2003**, *300*, 625−627.
(16) Adamcick, J.; Berquand, A.; Mezzenga, R. *Appl. Phys. Lett.* **2011**, *98*, 1937011−1937013.
(17) Byrne, N.; Hameed, N.; Werzer, O.; Quo, G. *Eur. Polym. J.* **2011**, *47*, 1279−1283.
(18) Smith, J. F.; Knowles, T. P. J.; Dobson, C. M.; MacPhee, C. E.; Welland, M. E. *Proc. Natl. Acad. Sci. U.S.A.* **2006**, *103*, 15806−15811.
(19) Hamley, I. W.; Kryssmann, M. J. *Langmuir* **2008**, *24*, 8210−8214.
(20) Case, D. A.; et al. AMBER 9; University of California: San Francisco, CA, 2006.
(21) Berendsen, H. J. P.; Postma, J. P. M.; van Gusteren, W. F.; DiNola, A.; Haak, J. R. *J. Chem. Phys.* **1984**, *81*, 3684−3690.
(22) Ryckaert, J. P.; Ciccotti, G.; Berendsen, H. J. P. *J. Chem. Phys.* **1974**, *23*, 327−341.
(23) Toukmaji, A.; Sagui, C.; Board, J.; Darden, T. *J. Chem. Phys.* **2000**, *113*, 10913−10927.
(24) Jorgensen, W. L.; Chandrasekhar, J.; Madura, J. D.; Impey, R. W.; Klein, M. L. *J. Chem. Phys.* **1983**, *79*, 926−935.
(25) Phillips, J. C.; Braun, R.; Wang, W.; Gumbart, J.; Tajkhorshid, E.; Villa, E.; Chipot, C.; Skeel, R. D.; Kale, L.; Schulten, K. *J. Comput. Chem.* **2005**, *26*, 1781−1802.
(26) Kirkpatrick, S.; Vecchi, C. D.; Vecchi, M. P. *Science* **1983**, *220*, 671−680.
(27) Zanuy, D.; Flores-Ortega, A.; Casanovas, J.; Curco, D.; Nussinov, R.; Alemán, C. *J. Phys. Chem. B* **2008**, *112*, 8692−8700.
(28) MacQueen, J. B. In Some methods for classification and analysis of multivariate data. *Proc. 5th Berkeley symposium on Math, Statistics, and Probability*; University of California Press 1967; pp 281−297.
(29) Revilla-López, G.; Torras, J.; Nussinov, R.; Alemán, C.; Zanuy, D. *Phys. Chem. Chem. Phys.* **2011**, *13*, 9986−9994.
(30) Blomqvist, J.; Mannfors, B.; Pietilä, L.-O. *J. Mol. Struct THEOCHEM* **2000**, *531*, 359−374.
(31) Humphrey, W.; Dalke, A.; Schulten, K. *J. Mol. Graph. Model.* **1996**, *14*, 33−38.
(32) Pettersen, E. F.; Goddard, T. D.; Huang, C. C.; Couch, G. S.; Greenblatt, D. M.; Meng, E. C.; Ferrin, T. E. *J. Comput. Chem.* **2004**, *25*, 1605−1612.

(33) Härd, T. *FEBS J.* **2011**, *278*, 3884−3892.
(34) Liu, K.; Cho, H. S.; Lashuel, H. A.; Kelly, J. W.; Wemmer, D. E.. *Nat. Struct. Biol.* **2000**, *7*, 754−757.
(35) McParland, V. J.; Kalverda, A. P.; Homans, S. W.; Radford, S. E. *Nat. Struct. Biol.* **2002**, *9*, 326−331.
(36) Perczel, A.; Angyán, J. G.; Kajtar, M.; Viviani, W.; Rivail, J. L.; Marcossia, J. F.; Ciszmadia, I. G. *J. Am. Chem. Soc.* **1991**, *113*, 6256−6265.
(37) Castelletto, V.; McKendrick, J. E.; Hamley, I. W.; Olsson, U.; Cenker, C. *Langmuir* **2010**, *26*, 11624−11627.
(38) Hamley, I. W.; Brown, G. D.; Castelletto, V.; Cheng, G.; Venanzi, M.; Caruso, M.; Placidi, E.; Alemán, C.; Revilla-Lopez, G.; Zanuy, D. *J. Phys. Chem. B* **2010**, *114*, 10674−10683.
(39) Castelletto, V.; Newby, G. E.; Zhu, Z.; Hamley, I. W.; Noirez, L. *Langmuir* **2010**, *26*, 9986−9996.
(40) Castelletto, V.; Newby, G. E.; Merino, D. H.; Hamley, I. W.; Liu, D.; Noirez, L. *Polym. Chem-UK* **2010**, *4*, 453−459.
(41) Stanley, C. B.; Perevozchikova, T.; Berthelier, V. *Biophys. J.* **2011**, *100*, 2504−2512.
(42) Andrews, M. N.; Winter, R.. *Biophys. Chem.* **2011**, *156*, 43−50.
(43) de la Torre, J. G.; Huertas, M. L.; Carrasco, B. *Biophys. J.* **2000**, *78*, 719−730.
(44) Zanuy, D.; Hamley, I. W.; Alemán, C. *J. Phys. Chem. B.* **2011**, *115*, 8937−8946.
(45) Curcó, D.; Revilla-López, G.; Alemán, C.; Zanuy, D. *J. Pept. Sci.* **2011**, *17*, 132−138.